Dalton Transactions

ROYAL SOCIETY OF CHEMISTRY

PAPER

View Article Online
View Journal | View Issue

Cite this: *Dalton Trans.*, 2024, **53**, 2678

Saccharide formation by sustainable formose reaction using heterogeneous zeolite catalysts†

Minoru Waki, * Soichi Shirai and Yoko Hase

The formose reaction is a unique chemical reaction for the preparation of saccharides from formaldehyde, a single carbon compound. We applied zeolite materials as heterogeneous catalysts to the formose reaction. The simple addition of Linde type A zeolite containing calcium ions (Ca-LTA) to an aqueous solution of formaldehyde and glycolaldehyde produced saccharides at room temperature. A quantitative analysis performed by high-performance liquid chromatography revealed that triose, tetrose, pentose, and hexose saccharides were produced with few byproducts. Ca-LTA was recovered from the reaction mixture by filtration, and the retrieved zeolite was found to be reusable under the same conditions. The catalytic activity of Ca-LTA was higher than those of conventional calcium catalysts and other solid materials such as silica, alumina, and hydroxyapatite. Several other types of zeolites with different crystal structures and alkali/alkali-earth metal ions also showed catalytic activity for saccharide formation. Based on the analytical results obtained by infrared spectroscopy, temperature-programmed desorption profiles and NMR measurements, we propose a reaction mechanism in which C–C bond formation is promoted by the mild basicity of the oxygen atoms and acidity on the metal ions of the aluminosilicate on the zeolite surfaces with low SiO_2/Al_2O_3 ratios.

Received 21st July 2023,
Accepted 19th December 2023

DOI: 10.1039/d3dt02321d

rsc.li/dalton

Introduction

Saccharides are important biomolecules, serving as a main energy source and a key component in nature with multiple roles in biological processes. Commercially available saccharides are produced from agricultural products such as sugarcane and sugar beets. With climate change causing global warming, if there is no improvement in the natural environment, agricultural yields will decrease in the near future. Additionally, consumption of sugars is increasing along with the global population. While sugar-derived biofuels are expected to be utilized as an alternative energy source to fossil fuels, these changes also lead to concern about food supply shortage. For sustainable development, it may be necessary to establish the artificial production of saccharides *via* non-agricultural approaches.[1] However, the chemical synthesis of saccharides is still challenging. The formose reaction, reported by Butlerow in 1861, is well-known as a series of chemical reactions that produce various saccharides from formaldehyde, a C1 compound.[2–5] The formose reaction produces a mixture of the following products by the oligomerization of formaldehyde (C1) under basic conditions: C5 and C6 saccharides, sugar alcohols, and intermediate products such as glycolaldehyde (C2), glyceraldehyde ($C3_{ald}$), dihydroxyacetone ($C3_{ket}$), aldotetrose ($C4_{ald}$), and ketotetrose ($C4_{ket}$) (Scheme 1). These intermediate products are formed by a cascade reaction consisting of the aldol reaction, reverse-aldol reaction, and Lobry de Bruyn-van Ekenstein transformation as proposed by Breslow in 1959.[6]

A variety of inorganic salts, containing Ca^{2+}, Mg^{2+}, and Ba^{2+} ions, have been applied as homogeneous catalysts for the

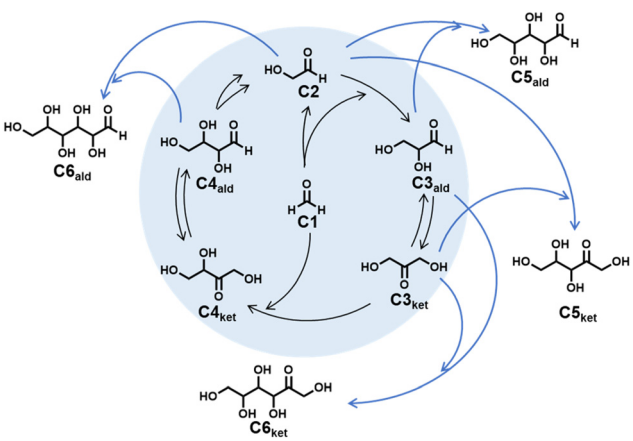

Scheme 1 Saccharide formation from formaldehyde and glycolaldehyde by the formose reaction.

Toyota Central R&D Labs., Inc., 41-1, Yokomichi, Nagakute, Aichi, Japan.
E-mail: mwaki@mosk.tytlabs.co.jp; Tel: +81-561-71-7169

†Electronic supplementary information (ESI) available: Additional reaction trials, ^{13}C, ^{27}Al MAS, ^{29}Si DD-MAS NMR, TPD, HPLC analysis. Computational conditions and detailed calculation results. See DOI: **https://doi.org/10.1039/d3dt02321d**

formose reaction.[4] The active catalysts transform C1 to saccharides with linear structures, while a large number of byproducts other than linear saccharides are simultaneously produced. C–C bond formations at secondary carbons of substrates give a variety of branched saccharides. Two molecules of C1 are disproportionated to formic acid and methanol in the Cannizzaro reaction under basic conditions.[7,8] Other inorganic salts and metal oxides such as TlOH, CrO_3, CdO, and $Pb(OH)_2$ also exhibit catalytic activities;[3,4,9–11] however, they present a crucial risk of inducing water pollution due to their biological toxicity.

Heterogeneous catalysts have been employed to express reactivity and selectivity originating at specific sites on the solid surface. The easy removability of heterogeneous catalysts from reaction solutions has attracted attention from the point of view of green chemistry.[12–14] For example, apatite, a group of phosphate minerals, was applied to the formose reaction as a solid catalyst.[15,16] Saccharide formation using carbonate apatite was achieved in a heterogeneous system under basic conditions. In another case, Okamoto and Usami reported a one-pot pentose formation from C1 and C2 starting materials using hydroxyapatite (HAP) as a catalyst.[17,18] The reaction proceeded in the presence of HAP without pH control. However, pentose formation with HAP required a high reaction temperature, 80 °C, and a quantitative discussion of reaction efficiency was difficult due to the presence of various byproducts.

Zeolites are among the most functional heterogeneous catalysts with high surface areas and uniformly nano-sized pores for molecular diffusion.[19–32] Aluminosilicates are the main crystalline components in the zeolite framework, showing high thermal stability. The acidity and basicity attributed to the aluminosilicate are known to function as active sites in acid/base reactions, and some zeolites have been reported to exhibit catalytic activity for C–C coupling based on the aldol reaction. Tetrose formation was achieved using C2 or C3 compounds with Lewis acidic zeolites, which promoted enolization of the substrates.[19,22–24] There is a large number of reports with regard to acidic and/or basic zeolites for the aldol reaction, although the use of catalysts for the formose reaction has been limited. The formose reaction for saccharide production using zeolites in the previous reports required high temperature,[33] alkaline media,[34] or gamma-ray irradiation.[35] However, a zeolite has been used as a solid support for a thiazolium catalyst, which promoted the formose reaction in an organic solvent.[36] The Cannizzaro reaction and the decomposition of products and catalysts under such harsh conditions decreased the reaction efficiency for forming saccharides. Therefore, optimization of reaction conditions and clarifying the reaction process on the surface of zeolites are important in order to improve their catalytic activity for the formose reaction.

In this study, we report a sustainable formose reaction using a Linde type A zeolite having calcium cations (Ca-LTA) in aqueous media at room temperature without the addition of a secondary alkali source. Ca-LTA exhibited catalytic activity to form triose (C3), tetrose (C4), pentose (C5), and hexose (C6) from C1 and C2 starting materials with high conversion and production yield, indicating that few byproducts were found. Addition of C2 as a starting material can shorten the specific induction period for the reaction to proceed. The catalyst was easily recovered by filtration from the reaction mixture and reused as a catalyst for the formose reaction under the same conditions. The catalytic activity of Ca-LTA was higher than those of conventional catalysts such as calcium inorganic salts, silica, alumina, and hydroxyapatite under the present conditions. Other types of zeolites with alkali/alkali-earth metal cations having different crystal structures also showed catalytic activity for saccharide production. High catalytic performance was characteristic of zeolites with low silica alumina ratios. The proposed reaction mechanism on the active site, based on the analytical results obtained by infrared (IR) spectra, temperature-programmed desorption (TPD) profiles and NMR studies, suggested that C–C bond formation was promoted by the mild acidity and basicity of the aluminosilicate on the solid surface.

Experimental section

Materials

All chemicals were purchased and used as received. Zeolites were obtained from Fujifilm Wako Pure Chemical Corporation and Tosoh Corporation. Linde type A zeolites are denoted with the code LTA, which contain potassium (K-LTA), sodium (Na-LTA), and calcium (Ca-LTA) as cations with pore diameters of 3, 4, and 5 Å, respectively. Faujasite zeolites are represented as type X (FAU-X) and Y (FAU-Y). Mordenite zeolites used are designated as the sodium form (Na-MOR) and hydrogen form (H-MOR). Linde type L, ferielite, MFI-type, and beta type are denoted as LTL, FER, ZSM-5, and BEA, respectively. The mesh sizes of these zeolites are 100 (K-LTA, Na-LTA, Ca-LTA, FAU-X, FAU-Y, Na-MOR, H-MOR, and FER) and 70 (LTL, BEA, and ZSM-5) mesh. Physical parameters including Brunauer–Emmett–Teller (BET) surface area (S_{BET}), pore diameter (D), and silica alumina ratio (SiO_2/Al_2O_3) are summarized in Table S1.†

General procedure for formose reaction using heterogeneous catalysts

Zeolite catalyst or conventional solid catalyst (300 mg) was added to an aqueous solution (10 mL) containing 0.15 M formaldehyde and 0.075 M glycolaldehyde (45 mg, 0.75 mmol). The mixture was stirred at room temperature for 72 h. Sample aliquots were collected at regular time intervals and filtered to remove the catalyst. The filtrate was subjected to high-performance liquid chromatography (HPLC) analysis to monitor the reaction.

General procedure for formose reaction using calcium inorganic salt catalysts

$Ca(OH)_2$ (22.2 mg, 0.3 mmol) or $Ca(OAc)_2$ (56 mg, 0.3 mmol)/NaOH (0.045 M) was added to an aqueous solution (10 mL) containing 0.15 M formaldehyde and 0.075 M glycolaldehyde (45 mg, 0.75 mmol). The mixture was stirred at room temperature for 72 h. Sample aliquots were collected at regular time intervals and treated with ion-exchange resin to remove the

calcium salt. The mixture was filtered to monitor the reaction by HPLC analysis.

HPLC analysis

To monitor C1, C2, C3 and C4 formation, reverse-phase HPLC analysis was performed on a JASCO system equipped with a GL Science Inertsil ODS-3 column (3.0 I.D. × 250 mm) at 40 °C. Acetonitrile/water (50 : 50 v/v) was used as the mobile phase solvent at a flow rate of 0.6 mL min^{-1}. Samples (2.4 μL) were diluted with water (1.18 mL) containing 30% phosphate acid (30 μL), followed by adding 2 mM 2,4-dinitrophenylhydrazine (DNPH)-acetonitrile solution (0.4 mL). An aliquot of 10 μL was injected into the HPLC system. Detection was conducted by UV/vis absorption at 360 nm.

C5 and C6 saccharides were detected by HPLC analysis using the arginine derivative method using a Shimadzu Nexera system equipped with a Shodex Asahipak NH_2-50 4E column (4.6 mm I.D. × 250 mm). Acetonitrile/water (95 : 5 v/v) including 3% phosphate acid was used as the mobile phase solvent with a flow rate of 0.8 mL min^{-1}. The temperature of the column oven was set at 40 °C. Arginine (29 mM)/boronic acid (0.4 M) solution containing 0.2 M KOH at a flow rate of 0.5 mL min^{-1} was used for transformation to the fluorescence derivatives in a chemical reactor bath at 150 °C. The sample (0.15 mL) was diluted with water (1.35 mL) and an aliquot of 10 μL was injected into the HPLC system. Detection was conducted by fluorescence emission at 430 nm (λ_{ex} = 320 nm). Concentrations were determined by calibration curves, which were obtained from five-point external standards. The reaction yields and conversions were calculated based on carbon-atom moles to evaluate the catalytic activity according to the following equations:

$$\text{Yield/C-mol\%} = \frac{n \times [Cn]}{[C1_{int}] + 2 \times [C2_{int}]} \times 100$$

where $[C1_{int}]$ and $[C2_{int}]$ are the initial concentrations of C1 and C2, respectively, and $[Cn]$ (n = 3–6) is the concentration of C3–C6 products observed during formose reactions.

$$\text{Conversion/C-mol\%} = \frac{([C1_{int}] + 2 \times [C2_{int}]) - ([C1] + 2 \times [C2])}{[C1_{int}] + 2 \times [C2_{int}]} \times 100$$

where [C1] and [C2] are concentrations of unreacted C1 and C2, respectively, during formose reactions.

Results and discussion

Performance for saccharide formation using Ca-LTA as a heterogeneous catalyst for formose reaction

The formose reaction was performed using Ca-LTA at room temperature in the presence of C1 and C2. The products were obtained as an aqueous complex mixture of saccharides. Separation of the products was prohibitively difficult due to their structural similarities and variety of stereoisomers. Thus, the analysis of the products was carried out by HPLC. The generation of $C3_{ald}$, $C3_{ket}$, $C4_{ald}$, and $C4_{ket}$ in the reaction mixture was confirmed by reverse-phase HPLC analysis using the DNPH derivative method (Fig. 1a).[37] C1 and C2 starting materials were consumed by the aldol reaction, and the amounts of C3 ($C3_{ald}$ and $C3_{ket}$) and C4 ($C4_{ald}$ and $C4_{ket}$) increased with the elapse of reaction time. C5 and C6 generated in the formose reaction were detected by HPLC analysis using the arginine derivative method.[38] Several intense peaks observed in the chromatograph of the reaction mixture after 24 h were assigned to $C5_{ket}$, $C5_{ald}$, and $C6_{ket}$ (Fig. 1b). A preliminary test using C2 and $C3_{ket}$ as starting materials with Ca-LTA showed preferable formation of $C5_{ket}$ species, which are ribulose (Ribu) and/or xylulose (Xylu) (Fig. S1†). Ribu and Xylu were not identified separately by this

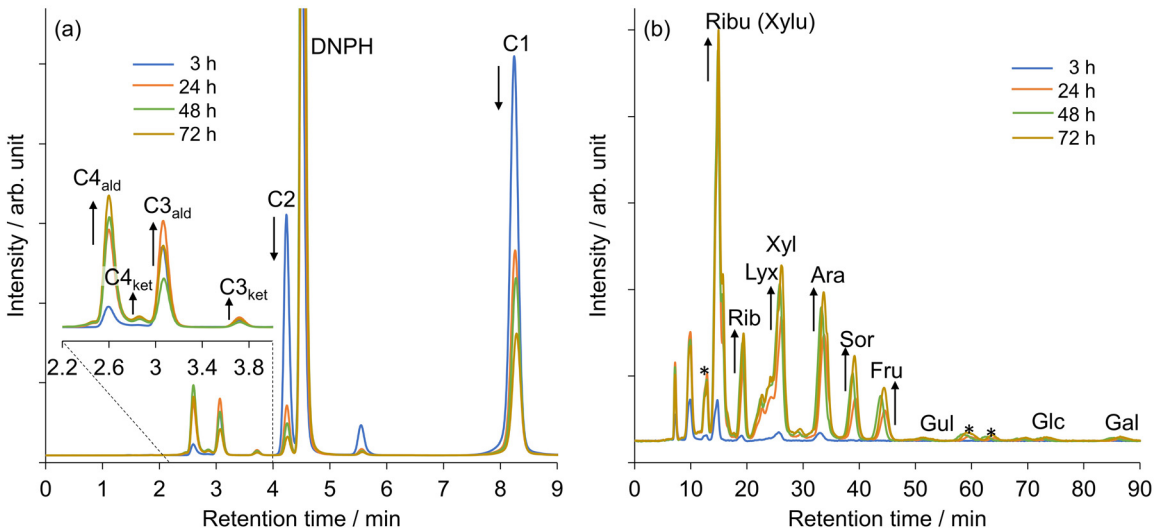

Fig. 1 Chromatograms obtained from formose mixture using Ca-LTA. (a) Reverse-phase HPLC analysis using DNPH derivative method and (b) normal-phase HPLC analysis using arginine derivative method. Asterisks indicate unidentified peaks.

Table 1 Catalytic activity of Ca-LTA under several conditions[a]

Entry	Catalyst	Mass/mg	Ca content/mmol	Temp./°C	Conv./C-mol%	Yield/C-mol%			
						C3	C4	C5	C6
1	Ca-LTA	300	1.14	25	75.0	15.6	48.6	5.6	1.8
2	Ca-LTA	100	0.38	25	67.4	20.5	41.2	4.6	1.1
3	Ca-LTA	30	0.11	25	45.7	22.1	21.0	1.8	0.2
4	No catalyst	—	—	25	16.9	0.04	0	0	0
5	Ca-LTA	300	1.14	5	37.2	20.1	15.8	1.3	0.1
6	Ca-LTA	300	1.14	60	98.5	1.5	14.7	9.1	5.2

[a] C1 = 0.15 M, C2 = 0.075 M, reaction time = 48 h.

analysis method. The combination of C2 and $C3_{ald}$ in the presence of Ca-LTA produced $C5_{ald}$, of which four epimers were assignable to ribose (Rib), lyxose (Lyx), xylose (Xyl), and arabinose (Ara) (Fig. S2†). These C5 products were observed in the mixture produced by the formose reaction of C1 and C2 with Ca-LTA (Fig. 1b), suggesting that C5 production can be expected from C2 and C3, as shown in Scheme 1. $C6_{ket}$ species observed in the formose mixture were assigned to sorbose (Sor) and fructose (Fru) (Fig. 1b), which were the main products obtained from $C3_{ald}$ and $C3_{ket}$ as starting materials (Fig. S3†). Gulose (Gul), glucose (Glc), and galactose (Gal) as $C6_{ald}$ products were observed in small amounts under the experimental conditions used.

The reaction conditions in the presence of Ca-LTA were optimized by changing the catalyst mass and the reaction temperature (Table 1). The formose reaction using 30 mg of Ca-LTA showed a lower yield of C3–C6 saccharides than 100 and 300 mg amounts of Ca-LTA (entries 1–3). In the absence of a catalyst, a large amount of C1 and C2 remained intact after 48 h, with almost no C3–C6 saccharide products (entry 4). The reaction temperature had a significant effect on the yield and conversion of the formose reaction using Ca-LTA. The formose reaction performed at 5 °C slowly produced C3–C6 saccharides, while the high temperature of 60 °C promoted the conversion of starting materials (C1 and C2) (entries 5 and 6). However, the products (C3–C6) were consumed and transformed to unidentifiable products at higher temperatures.

The conversion of starting materials and yields of C3–C6 products were plotted against reaction time (Fig. 2). The sum of the yields of C3–C6 gradually increased with reaction time and reached 71.6% at 48 h. The conversion was 75.0% for 48 h, suggesting that a few branched chain products and/or byproducts were formed with a yield of 3.4%. The unidentified peaks at 12, 60, and 65 min of retention time in the HPLC analysis using the arginine derivative system might correspond to the branched chain products (Fig. 1b). The detailed structures of the branched sugars could not be determined by this method. On the other hand, the Cannizzaro reaction is known to be an undesired side reaction, yielding sugar alcohols and sugar acids as byproducts. The presence of sugar acids in the reaction mixture was confirmed by ^{13}C NMR analysis. A characteristic peak for the carbon of a carboxylic acid group was observed at 171 ppm, whereas formic acid and glycolic acid

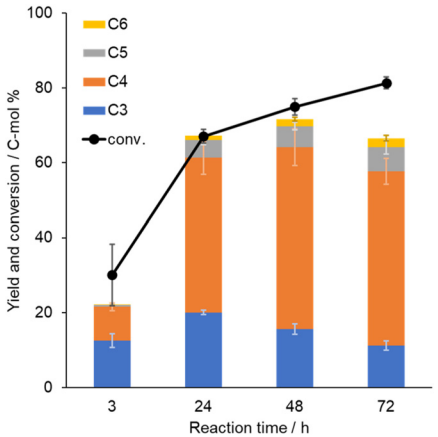

Fig. 2 Time course of conversion and yields of C3–C6 in formose reaction using Ca-LTA. Reaction conditions: C1 = 0.15 M, C2 = 0.075 M, Ca-LTA = 300 mg, Ca content = 1.14 mmol, H_2O = 10 mL, RT.

have their carboxylic acid carbons at 166 and 176 ppm, respectively (Fig. S4†). Therefore, the reaction mixture was likely to include some kind of sugar acid or α-keto acid with a carbon chain over 3.

In the conventional formose reaction under alkali conditions at high temperature (40–100 °C), C1 is wastefully consumed and affords formic acid and methanol by the Cannizzaro reaction, the disproportionation of C1.[5] Moreover, the harsh conditions cause fast degradation of saccharide products. Consequently, the conversion of C1 reaches nearly 100% in the conventional formose reaction. On the other hand, the conversion yield for starting materials (C1 and C2) increased to 75.0% under our conditions where Ca-LTA was used without other alkali sources at room temperature. The contribution of side reactions was only 3.4% at 48 h, while the production of C3–C6 was saturated (Fig. 2). Since all reaction steps for the formation of C2–C6 saccharides in the formose reaction are reversible in the proposed mechanism (Scheme 1), the overall reaction seems to reach an equilibrium between substrates (C1 and C2) and products (C3–C6). After 72 h, the total yield of products slightly decreased, while the conversion of C1 and C2 kept increasing. These observations implied that the generation of unidentified products proceeded in the solution after 48 h.

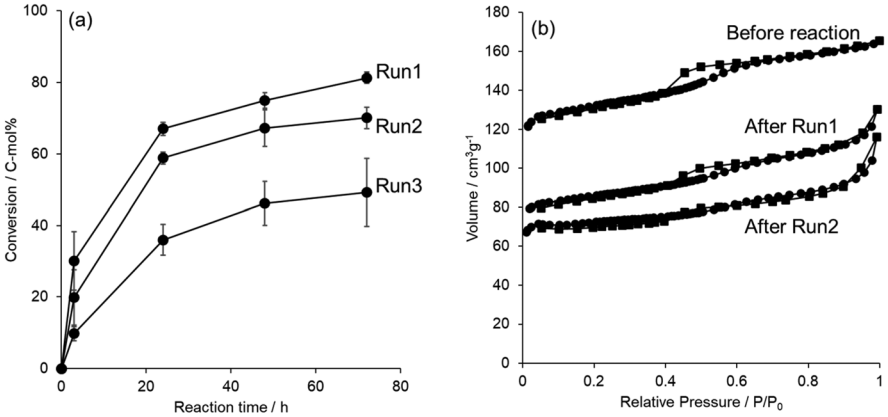

Fig. 3 (a) Reusability of Ca-LTA for formose reaction. Reaction conditions: C1 = 0.15 M, C2 = 0.075 M, Ca-LTA = 300 mg, H_2O = 10 mL, RT. (b) Nitrogen adsorption desorption isotherm for Ca-LTA before and after formose reaction.

The continuous increase in C3 and C4 compounds in Fig. 1a indicated that Ca-LTA promoted the aldol reaction that produced $C3_{ald}$ and $C4_{ket}$. In contrast, the other aldol reactions that generated C5 and C6 saccharides proceeded more slowly. These experimental observations were in accordance with theoretical calculation results. We carried out quantum chemical calculations employing the density functional theory (DFT) method[39] combined with conformational analysis.[40] The results indicated that the aldol reactions producing C5 and C6 saccharides were thermodynamically unfavorable (Fig. S5 and S6†). On the other hand, the concentration of C2 decreased continuously even though the DFT calculations suggested that the formation of C2 from $C4_{ald}$ was thermodynamically favorable (Fig. S5b†). These results revealed that Ca-LTA was less effective in promoting the reverse-aldol reaction to form C2 from $C4_{ald}$.

Next, the reusability of Ca-LTA was examined by recycling tests in which the catalyst was recovered by filtration and reused. The formose reaction by the used Ca-LTA successfully formed C3–C6 saccharides under identical conditions (Fig. 3a). The conversion was 81% for the first run after 72 h of reaction time, but 70% and 49% for the second and third runs, respectively, showing the conversion gradually decreased with the number of reuses. Nitrogen adsorption and desorption isotherms for the recovered Ca-LTA showed a slight decrease in the surface area and pore volume as shown in Fig. 3b and Table 2. The crystal structure of LTA was slightly damaged during the formose reaction, as confirmed by X-ray diffraction patterns (Fig. 4a). The intensity of the diffraction peak at 7.2° corresponding to the (200) planes of the cubic structure deceased to 69%. Thermogravimetric analysis (TGA) of the recovered catalyst showed a significant weight loss of 5% in the temperature range of 500–600 °C, which might be

Table 2 Textual parameters of zeolite catalyst before and after formose reaction

	S_{BET}/m^2 g^{-1}	$V_{t\text{-}plot}$/cm^3 g^{-1}
Before reaction	435	0.23
After run 1	284	0.14
After run 2	238	0.11

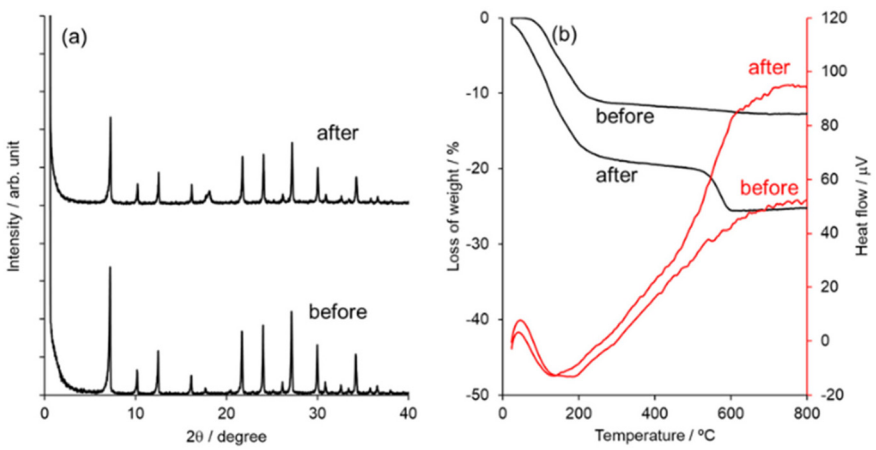

Fig. 4 (a) XRD patterns and (b) TG (black) and DTA (red) curves for Ca-LTA before and after formose reaction.

attributed to the organic compounds on the surface of Ca-LTA (Fig. 4b). To remove adsorbed residues, the zeolite catalyst recovered from the reusability test was washed in hot water using ultrasonics. The resulting eluent contained mainly C1, confirmed by HPLC analysis (Fig. S7†). These results suggested that a small amount of reaction substrates or products remained on the surface of the retrieved catalyst with partial collapse of the nanoporous structure, which resulted in a decrease in catalytic activity for subsequent runs using reused catalyst.

Formose reaction over other homogeneous and heterogeneous catalysts

Conventionally, calcium inorganic salts such as $Ca(OH)_2$ and $Ca(OAc)_2$ have been applied as catalysts for the formose reaction in basic solution. However, the use of these catalysts gave C3–C6 products with moderate yields of 48–55% for 0.5 h under our conditions, while the resulting mixture contained unidentified products as shown by the difference in conversion and C-mol yields (Fig. 5a). This was thought to be due to the significant consumption of C1 and C2 in the Cannizzaro and crossed Cannizzaro reactions under alkali conditions, resulting in the formation of byproducts. To investigate the influence of Ca^{2+} on catalytic activity, a Ca^{2+} supported ion-exchange resin (Ca-IER) was used in the formose reaction under the same conditions, which showed no activity for the formation of C3–C6 saccharides. Thus, calcium salts exhibited catalytic activity under basic conditions.

The catalytic activity of other solid catalysts was examined. In the previous report, hydroxyapatite (HAP) as a heterogeneous catalyst promoted the formose reaction of C1 and C2 substrates to produce ribose in aqueous solution at 80 °C.[17,18] However, HAP showed quite low activity for the formose reaction under ambient temperature (*ca.* 25 °C), indicating that it requires a high temperature to activate the coupling reaction of C1 and C2 (Fig. 5a). Silica, which is composed of a siloxane network, induced a small amount of products from C1 and C2. α-Alumina, which is composed of an aluminum oxide network, also exhibited low activity for the formose reaction (Fig. 5a). However, γ-alumina was found to be an effective catalyst for the formose reaction with a moderate yield of 37%, but this was still lower than for of zeolite Ca-LTA (Fig. 5a). These results suggested that zeolite has specific activity for the formose reaction, which was higher than pure silica and pure alumina, indicating that the aluminosilicate structure of zeolite plays an important role in the reaction promotion.

Various types of zeolites having other crystal structures and cations were applied to the formose reaction as heterogeneous catalysts (Fig. 5b). K-LTA and Na-LTA exhibited catalytic activities similar to Ca-LTA for the reactions. The conversions for K-LTA and Na-LTA were 80% and 83%, respectively, in the reaction time of 48 h, which were higher than that of Ca-LTA. However, the production yield of C3–C6 was 67% for K-LTA, which was lower than that with Ca-LTA. Na-LTA showed a good activity for the generation of C3–C6 with a high yield of 72%, but the unidentified products including branched chain saccharides and byproducts were formed with a yield of 11%. These results indicated that the difference in the cation in the framework of LTA affected the catalytic activity. FAU-X generated C3–C6 products in high yields, similar to that of LTA. FAU-Y gave a lower reaction yield than FAU-X.

However, the production yields of C3–C6 were 66% for both K-LTA and Na-LTA, which were lower than that with Ca-LTA, indicating that the difference in the cation in the framework of LTA affected the catalytic activity. FAU-X generated C3–C6 products in high yields, similar to that of LTA. FAU-Y gave a lower reaction yield than FAU-X.

Focusing on the Si/Al ratio for the zeolites shown in Table S1,† a correlation between the SiO_2/Al_2O_3 ratio and catalytic activity was suggested as follows. LTAs and FAU-X, which showed high activity for the formose reaction (conversion > 80%), had low SiO_2/Al_2O_3 ratios (SiO_2/Al_2O_3 < 3). Zeolite catalysts having SiO_2/Al_2O_3 ratios between 5–18, such as FAU-Y, LTL, Na-MOR, and FER, showed moderate activity for the reac-

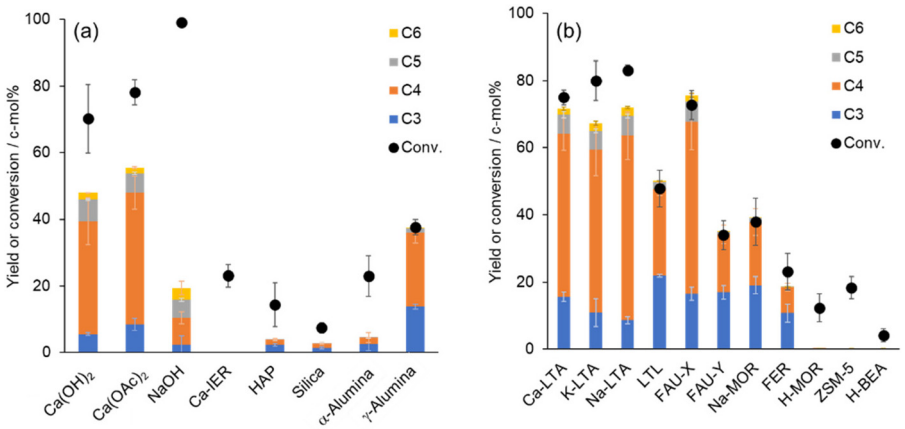

Fig. 5 Yield and conversion in formose reaction using (a) conventional catalysts and (b) other types of zeolites. Reaction conditions: C1 = 0.15 M, C2 = 0.075 M, $Ca(OH)_2$ = 0.03 M, $Ca(OAc)_2$ = 0.03 M with NaOH of 0.045 M, other solid catalysts = 300 mg, H_2O = 10 mL, RT, 0.5 h ($Ca(OH)_2$, and $Ca(OAc)_2$) or 48 h (other catalysts).

tion with conversion yields ranging from 23–48%. In contrast, zeolites including silica in high ratios (SiO_2/Al_2O_3 = 50–360), such as BEA, H-MOR, and ZSM-5, showed little activity and gave smaller amounts of C3 and C4 products. The properties of these series of zeolites indicated that zeolite catalysts with low SiO_2/Al_2O_3 ratios were effective for promoting the production of C3–C6 saccharides at room temperature.

Characterization of catalytic active sites

To clarify the unique activity of the zeolite catalyst for the formose reaction, the catalytic active sites on the aluminosilicate framework were investigated. TPD profiles were measured by using NH_3 and CO_2 as probe molecules to evaluate the acidity and basicity of Ca-LTA. NH_3-TPD showed a desorption peak in the range of 100–300 °C due to the physisorption of NH_3 on the solid surface (Fig. S8a†). No characteristic peak was observed in the high-temperature range around 400–600 °C, indicating that Ca-LTA does not have Brønsted acid sites on its surface. The CO_2-TPD profile exhibited an intense signal at 592 °C attributed to CO_2 adsorption on the basic sites (Fig. S8b†). These TPD profiles clearly showed that Ca-LTA has a basic character. IR spectra of Ca-LTA using a pyridine probe are shown in Fig. 6. No peak arising from Brønsted acids was observed around 1560 cm^{-1}, which is in good agreement with the TPD result. On the other hand, characteristic peaks were observed at 1454 and 1487 cm^{-1} immediately after treatment with pyridine, which were attributed to adsorption on Lewis acidic sites of Ca-LTA. After heating to remove excess physisorbed pyridine, the peaks remained in this region but became quite small. This suggested that extremely weak Lewis acidic sites existed on the surface of Ca-LTA.

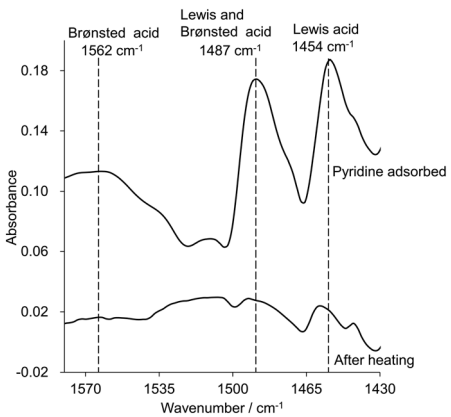

Fig. 6 FT-IR spectra of Ca-LTA using pyridine as probe molecule.

In ^{27}Al magic-angle-spinning (MAS) NMR measurements, the chemical shift reflects the electronic state of Al atoms in the Ca-LTA zeolite framework.[41–43] The ^{27}Al NMR spectrum showed an intense peak at 54 ppm with spinning side bands corresponding to tetrahedrally coordinated Al^{IV} (Fig. 7a). The lack of octahedrally coordinated Al^{VI} signals around 0 ppm indicated that extra-framework aluminum species were absent in Ca-LTA. Thus, Ca-LTA has no Al species that function as Lewis acidic sites. Another signal observed at 82 ppm was assigned to $Al(OH)_4^-$, which may be aluminum raw materials from the synthesis of Ca-LTA.[44] ^{27}Al MAS NMR spectra of other zeolites such as K-LTA, Na-LTA, and FAU-X, which also showed high activity for the formose reaction, showed a single peak in the range of 50–60 ppm without peaks around 80 ppm (Fig. S9†). The spectra suggested that K-LTA, Na-LTA, and FAU-X have tetrahedral Al^{IV} in the framework without Al $(OH)_4^-$. Despite the absence of $Al(OH)_4^-$, the formose reaction using these zeolites as catalysts produced C3–C6 saccharides in high yield. Therefore, these results indicated that $Al(OH)_4^-$ contamination in Ca-LTA did not affect the catalytic activity of Ca-LTA for the formose reaction. The ^{29}Si dipolar-decoupling (DD)-MAS NMR spectrum of Ca-LTA showed two resonance peaks at −90 and −96 ppm assigned to $Si(OSi)(OAl)_3$ and Si $(OSi)_2(OAl)_2$, respectively (Fig. 7b). No silanol signals were found at lower magnetic field, indicating that the effect of Si-OH species on the surface of Ca-LTA was negligible during the catalytic reaction. After the reaction, the recovered Ca-LTA took the C1 substrate into the pores, as confirmed by TGA (Fig. 4b) and a washing test (Fig. S7†) of recovered Ca-LTA. To obtain information about the adsorption mechanism, ^{27}Al MAS and

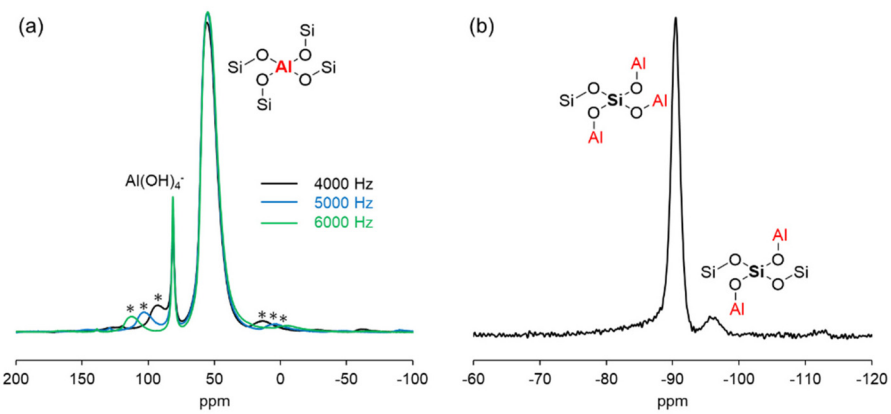

Fig. 7 (a) ^{27}Al and (b) ^{29}Si MAS NMR spectra of Ca-LTA. Asterisks indicate spinning side bands.

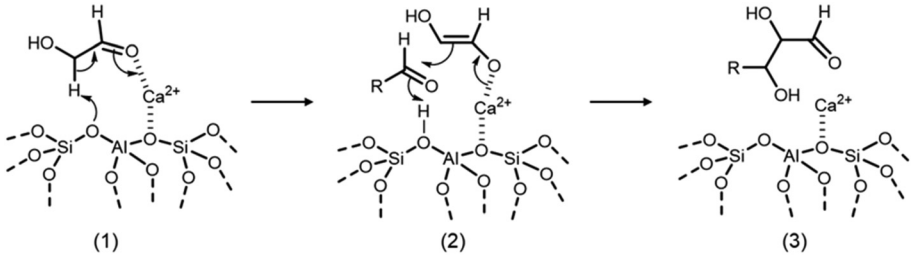

Scheme 2 Proposed mechanism for C–C bond formation during formose reaction using Ca-LTA.

^{29}Si DD-MAS NMR spectra of recovered Ca-LTA including absorbed C1 were measured; however, these spectra were identical to those of Ca-LTA before the reaction, indicating that local adsorption of the substrate on the surface had little effect on the electronic state of the framework (Fig. S10†).

Based on these results, a reaction mechanism on Ca-LTA was proposed as follows. Generally, the aldol reaction in the formose reaction can be achieved by a base-catalyzed mechanism *via* an enolate intermediate. Ca-LTA has base and Lewis acid sites on its surface, as confirmed by the TPD and IR measurements. The basicity and Lewis acidity of Ca-LTA play an important role in generation of the enolate from an aldehyde having an α-proton. It is generally accepted that the basicity of zeolites is due to the electronegativity of the framework oxygen atom.[45–48] Meanwhile, alkali and alkaline-earth metal cations perform as Lewis acid sites, according to previous reports.[49–53] Thus, in our proposed mechanism, the lattice oxygen of Ca-LTA serves as a Brønsted base site for deprotonation to form the enolate in combination with the Lewis acidity of the Ca^{2+} cation in the framework as shown in Scheme 2 (**1**). The formed enolate attacks another aldehyde to form a C–C bond (**2**), followed by proton transfer from the protonated lattice oxygen to the alkoxide to form the aldol product (**3**). The surface structure of the zeolite then returns to its original state. This cooperative mechanism between basicity and Lewis acidity is thought to be accelerated on zeolite surfaces with low SiO_2/Al_2O_3 ratios. Similar mechanisms for the generation of enolates using Lewis acidic zeolites have been reported in the literature. The framework oxygen acts as a base to abstract the α-proton in concert with the Lewis acidity of the zeolites, which promotes enolization of carbonyl substrates following C–C coupling in the aldol reaction.[19,22–24] Thus, we believe that our proposed mechanism for C–C formation in the formose reaction using Ca-LTA is plausible.

Conclusions

We performed the formose reaction using zeolites as heterogeneous catalysts in aqueous medium at room temperature. Formaldehyde and glycolaldehyde were successfully converted to triose, tetrose, pentose and hexose with high conversion in the presence of few byproducts, representing a unique reaction mechanism of an acid–base cooperative system on a solid surface. These properties are favorable from the viewpoint of green chemistry and would be useful for future industrial processes.

Author contributions

MW carried out all the experiments. YH and SS performed the theoretical calculations. All authors contributed to writing the manuscript.

Conflicts of interest

There are no conflicts to declare.

Acknowledgements

The authors thank Dr Yasutomo Goto for measuring the solid-state NMR spectra.

References

1 C. P. O'Brien, M. J. Watson and A. W. Dowling, *ACS Energy Lett.*, 2022, **7**, 3509–3523.
2 A. Butlerow, *Justus Liebigs Ann. Chem.*, 1861, **120**, 295–298.
3 T. Mizuno and A. H. Weiss, Synthesis and Utilization of Formose Sugars, in *Advances in Carbohydrate Chemistry and Biochemistry*, ed. R. S. Tipson and D. Horton, Academic Press, New York and London, 1974, vol. 29, pp. 173–227.
4 Z. Iqbal and S. Novalin, *Curr. Org. Chem.*, 2012, **16**, 769–788.
5 I. V. Delidovich, A. N. Simonov, O. P. Taran and V. N. Parmon, *ChemSusChem*, 2014, **7**, 1833–1846.
6 R. Breslow, *Tetrahedron Lett.*, 1959, **1**, 22–26.
7 H. Tambawala and A. H. Weiss, *J. Catal.*, 1972, **26**, 388–400.
8 R. F. Socha, A. H. Weiss and M. M. Sakharov, *J. Catal.*, 1981, **67**, 207–217.
9 T. I. Khomenko, M. M. Sakharov and O. A. Golovina, *Russ. Chem. Rev.*, 1980, **49**, 570–584.
10 E. Pfeil and G. Schroth, *Chem. Ber.*, 1952, **85**, 293–307.
11 Y. Shigemasa, M. Kawahara, C. Sakazawa, R. Nakashima and T. Matsuura, *J. Catal.*, 1980, **62**, 107–116.
12 Y. Román-Leshkov and M. E. Davis, *ACS Catal.*, 2011, **1**, 1566–1580.

13 G. Li, B. Wang and D. E. Resasco, *ACS Catal.*, 2020, **10**, 1294–1309.
14 S. De, A. Dokania, A. Ramirez and J. Gascon, *ACS Catal.*, 2020, **10**, 14147–14185.
15 C. Reid and L. E. Orgel, *Nature*, 1967, **216**, 455.
16 A. W. Schwartz and R. M. de Graaf, *J. Mol. Evol.*, 1993, **36**, 101–106.
17 K. Usami and A. Okamoto, *Org. Biomol. Chem.*, 2017, **15**, 8888–8893.
18 K. Usami, K. Ziao and A. Okamoto, *ACS Sustainable Chem. Eng.*, 2019, **7**, 3372–3377.
19 M. Dusselier, P. V. Wouwe, S. D. Smet, R. D. Clercq, L. Verbelen, P. V. Puyvelde, F. E. D. Prez and B. F. Sels, *ACS Catal.*, 2013, **3**, 1786–1800.
20 A. Primo and H. Garcia, *Chem. Soc. Rev.*, 2014, **43**, 7548–7561.
21 J. D. Lewis, S. V. D. Vyver and Y. Román-Leshkov, *Angew. Chem., Int. Ed.*, 2015, **54**, 9835–9838.
22 S. V. D. Vyver, C. Odermatt, K. Romero, T. Prasomsri and Y. Román-Leshkov, *ACS Catal.*, 2015, **5**, 972–977.
23 D. Palagin, V. L. Sushkevich and I. I. Ivanova, *J. Phys. Chem. C*, 2016, **120**, 23566–23575.
24 S. Tolborg, S. Meier, S. Saravanamurugan, P. Fristrup, E. Taarning and I. Sadaba, *ChemSusChem*, 2016, **9**, 3054–3061.
25 V. Verdoliva, M. Saviano and S. De Luca, *Catalysis*, 2019, **9**, 248.
26 D. Kerstens, B. Smeyers, J. V. Waeyenberg, Q. Zhang, J. Yu and B. F. Sels, *Adv. Mater.*, 2020, **32**, 2004690.
27 T. T. Le, A. Chawla and J. D. Rimer, *J. Catal.*, 2020, **391**, 56–68.
28 S. Ghosh, S. S. Acharyya, Y. Yoshida, T. Kaneko and Y. Iwasawa, *ACS Appl. Mater. Interfaces*, 2022, **14**, 18464–18475.
29 Y. Naresh, A. Shrotri and A. Fukuoka, *ACS Catal.*, 2022, **12**, 3534–3542.
30 N. Katada, K. Yamamoto, M. Fukui, K. Asanuma, S. Inagaki, K. Nakajima, S. Suganuma, E. Tsuji, A. Palcic, V. Valtchev, P. St Petkov, K. Simeonova, G. N. Vayssilov and Y. Kubota, *Microporous Mesoporous Mater.*, 2022, **330**, 111592.
31 R. Prajapati, D. Jadav, M. Pandey, K. Nishimura, S. Inagaki, Y. Kubota, R. Bandyopadhyay and M. Bandyopadhyay, *Eur. J. Inorg. Chem.*, 2022, e202200185.
32 P. Xiao, Y. Wang, Y. Lu, T. D. Baerdemaeker, A.-N. Parvulescu, U. Muller, D. D. Vos, X. Meng, F.-S. Xiao, W. Zhang, B. Marler, U. Kolb, H. Gies and T. Yokoi, *Appl. Catal., B*, 2023, **325**, 122395.
33 S. Trigerman, E. Biron and A. H. Weiss, *React. Kinet. Catal. Lett.*, 1977, **6**, 269–274.
34 A. H. Weiss, S. Trigerman, G. Dunells, V. A. Likholobov and E. Biron, *Ind. Eng. Chem. Process Des. Dev.*, 1979, **3**, 522–527.
35 S. Irie, *Chem. Lett.*, 1984, **13**, 2153–2156.
36 H. Tajima, K. Tabata, T. Niitsu and H. Inoue, *J. Chem. Eng. Jpn.*, 2002, **35**, 564–568.
37 M. Haas, S. Lamour and O. Trapp, *J. Chromatogr. A*, 2018, **1568**, 160–167.
38 H. Mikami and Y. Ishida, *Bunseki Kagaku*, 1983, **32**, E207–E210.
39 M. J. Frisch, G. W. Trucks, H. B. Schlegel, G. E. Scuseria, M. A. Robb, J. R. Cheeseman, G. Scalmani, V. Barone, G. A. Petersson, H. Nakatsuji, *et al.*, *Gaussian 16, Revision C.01*, Gaussian, Inc., Wallingford CT, 2016.
40 Promethium, **https://www.promethium.qcware.com**, QC Ware Corp., September 2023.
41 M. Haouas, F. Taulelle and C. Martineau, *Prog. Nucl. Magn. Reson. Spectrosc.*, 2016, **94–95**, 11–36.
42 J. Klinowski, *Chem. Rev.*, 1991, **91**, 1459–1479.
43 T. Yokoi, H. Mochizuki, S. Namba, J. N. Kondo and T. Tatsumi, *J. Phys. Chem. C*, 2015, **119**, 15303–15315.
44 B. C. Faust, W. B. Labiosa, K. H. Dai, J. S. Macfall, B. A. Browine, A. A. Ribeiro and D. D. Richter, *Geochim. Cosmochim. Acta*, 1995, **59**, 2651–2661.
45 D. Barthomeuf, *Catal. Rev. Sci. Eng.*, 1996, **38**, 521–612.
46 T. C. Keller, S. Isabettini, D. Verboekend, E. G. Rodrigues and J. Pérez-Ramírez, *Chem. Sci.*, 2014, **5**, 677–684.
47 J. N. Kondo, H. Yamazaki, R. Osuga, T. Yokoi and T. Tatsumi, *J. Phys. Chem. Lett.*, 2015, **6**, 2243–2246.
48 R. Osuga, T. Yokoi and J. N. Kondo, *J. Catal.*, 2019, **371**, 291–297.
49 H. Föster and M. Schumann, *J. Chem. Soc., Faraday Trans. 1*, 1989, **85**, 1149–1158.
50 H. Knözinger and S. Huber, *J. Chem. Soc., Faraday Trans.*, 1998, **94**, 2047–2059.
51 R. C. Deka and K. Hirao, *J. Mol. Catal. A: Chem.*, 2002, **181**, 275–282.
52 P. Mondal, H. A. Deka and R. C. Deka, *Mol. Simul.*, 2008, **34**, 1121–1128.
53 D. Bonenfant, M. Kharoune, P. Niquette, M. Mimeault and R. Hausler, *Sci. Technol. Adv. Mater.*, 2008, **9**, 013007.